Eur. Phys. J. B **59**, 115–126 (2007)
DOI: 10.1140/epjb/e2007-00272-6

THE EUROPEAN PHYSICAL JOURNAL B

Local v/a variations as a measure of structural packing frustration in bicontinuous mesophases, and geometric arguments for an alternating Im$\overline{3}$m (I-WP) phase in block-copolymers with polydispersity*

G.E. Schröder-Turk[1,2,a], A. Fogden[2], and S.T. Hyde[2]

[1] Institut f. Theoret. Physik I, Friedrich-Alexander-Universität Erlangen-Nürnberg, Staudtstr. 7, 91054 Erlangen, Germany
[2] Dept. of Applied Maths, Research School of Physical Sciences, Australian National University, Canberra 0200 ACT, Australia

Received 6 June 2007
Published online 5 October 2007 –

Abstract. This article explores global geometric features of bicontinuous space-partitions and their relevance to self-assembly of block-copolymers. Using a robust definition of 'local channel radius', based on the concept of a medial surface [1], we relate radius variations of the space-partition to polymolecular chain stretching in bicontinuous diblock- and terblock copolymer assemblies. We associate local surface patches with corresponding cellular volume elements, to define local volume-to-surface ratios. The distribution of these v/a ratios and of the channel radii are used to quantify the degree of packing frustration of molecular chains as a function of the specific bicontinuous geometry, modelled by triply-periodic minimal surfaces and related parallel interfaces. The Gyroid geometry emerges as the most nearly homogeneous bicontinuous form, with the smallest heterogeneity of channel radii, compared to the cubic Primitive and Diamond surfaces. We clarify a geometric feature of the Gyroid geometry: the three-coordinated nodes of the graph are *not* the widest points of the labyrinths; the widest points are at the midpoints of the edges. We also explore a more complex cubic triply-periodic surface, the I-WP surface, containing two geometrically distinct channel subdomains. One of the two channel systems is nearly as homogeneous in local channel diameters as the Gyroid, the other is more heterogeneous than the Primitive surface. Its hybrid nature suggests the possibility of an "alternating I-WP" phase in polydisperse linear ABC-terpolymer blends, with monodisperse molecular weight distributions (MWD) in the A and B blocks and a more polydisperse C block.

PACS. 02.40.-k Geometry, differential geometry, and topology – 61.30.St Lyotropic phases – 81.16.Dn Self-assembly – 82.35.Jk Copolymers, phase transitions, structure

1 Introduction

The self-assembly of AB block-copolymers into the complex $Ia\overline{3}d$ double-Gyroid phase is well-understood [2,3]. The mutually immiscible covalently bound blocks cannot phase-separate macroscopically; instead the components form microdomains. Assuming complete immiscibility (the strong-segregation limit of standard polymer theory), the domains are separated by two-dimensional walls, called the inter-material dividing surfaces (IMDS). That segregation is driven by competing physical constraints. The immiscibility of the two moieties imposes surface tension at the walls; second, the block chains seek to maximise their configurational entropy. Surface tension acts to reduce the wall area. In order to maintain the chain density in each domain at its bulk value, that shrinkage can only be accommodated by stretching individual polymer coils normal to the walls, reducing their entropy. That entropy loss is restored somewhat by curving the domain walls in order to reduce the stretch. The resulting global domain structure balances the entropic contributions induced by wall curvature against the effective surface tension. The final result is a structure that admits as uniform a distribution of domain dimensions and curvatures as possible, minimising the local and global chain packing frustration. Among the hyperbolic wall geometries, IMDS related to the low genus cubic triply-periodic

* Abbreviations used throughout this article: CMC: constant mean curvature, IMDS: inter-material dividing surface, TPMS: triply-periodic minimal surface, MS: medial surface, K: Gaussian curvature, H: mean curvature, SCFT: self-consistent field theory, LG: labyrinth graph, MWD: molecular weight distribution, PDI: polydispersity index.

[a] e-mail: Gerd.Schroeder-Turk@physik.uni-erlangen.de

minimal surfaces minimise curvature variations. The cubic Gyroid represents the least frustrated geometry among the complex bicontinuous phases, whose IMDS are hyperbolic [4]. Indeed, it is now widely accepted that, of the known cubic bicontinuous structures, monodisperse AB copolymers only form the cubic Gyroid structure of symmetry $Ia\overline{3}d$. Furthermore, only the double-Gyroid geometry with two intertwined labyrinths of moiety B separated by a matrix (or curved layer) of moiety A occurs; an *alternating* $I4_132$ Gyroid phase (with moiety A forming one labyrinthine domain, and B the other) has never been observed in diblock copolymers.

Despite our apparent progress, a robust quantitative estimate of the degree of packing frustration is, so far, lacking. The problem is far from simple. For example, the physical assembly is likely to deviate somewhat from the most tractable candidate geometries, such as constant mean curvature (CMC) surfaces (that are optimal under the action of surface tension alone) and surfaces exhibiting domains of uniform thickness (favoured by chain entropy). A better approach would explore a wider spectrum of candidate geometries. Detailed geometric analyses are however currently impossible in general cases. We do not pretend to attack that problem here. Rather, we develop a quantitative measure of packing frustration in general and then apply that to a restricted class of geometries, based on parallel surfaces to triply-periodic minimal surfaces.

Matsen and Bates quantified the packing frustration by the degree of deviation of the structure from its analogous CMC surface, measured by the standard deviation of the mean curvature [5]. Jinnai et al. experimentally measured interfacial curvature and demonstrated the deviations of the IMDS from CMC surface [6]. Later quantitative measures of packing homogeneity in complex bicontinuous geometries are plagued by the lack of a robust point-wise definition of *channel radius*. This parameter offers a direct measure of chain dimensions found in a particular geometry; it is also related to the assignation of domain volumes to a particular patch of the dividing surface in the bicontinuous geometry. Earlier analyses of this issue have relied on mappings from the hyperbolic surfaces within the bicontinuous morphology onto one-dimensional "labyrinth graphs" that lie at the core of the domains [7,8]. This focus on the labyrinth graph has led, for example, to a supposed correlation between the valency or degree of graph vertices and relative stability of the related bicontinuous geometry. The connection arises due to a purported link between graph degree (the edge valency at each node) and radius variations in the related structure. Thus, the three- and four-valent nodes in the cubic Gyroid and Diamond geometries respectively explain the formation of a Gyroid rather than Diamond morphology (e.g. [9]), assuming that a degree-four node incurs larger diameter variations than a degree-three node. We provide here a more rigorous definition of channel radii, that relies on a (two-dimensional) medial surface (MS) construction, rather than a (one-dimensional) labyrinth graph [1,4], see Section 2. The MS approach circumvents fundamental difficulties associated with the definition of a labyrinth graph. It allows for example comparison of the P, D and G geometries with the more complex bicontinuous structure based on the I-WP triply-periodic minimal surface, containing two distinct labyrinth graphs. We shall show that the I-WP has a very uniform labyrinth of degree four, with channels whose radii are of similar homogeneity to the degree-three Gyroid labyrinth channels (see Sect. 5). Our analysis is geometrically rigorous, offering a useful characterisation of candidate geometries without delving too deeply into the details of polymer chain energetics. Our approach is therefore a useful adjunct to more specific polymer theories. For example, while reference [7] explains the likely actual relative stability of the Primitive, Diamond and Gyroid geometries, that approach would presumably fail to recognise the likely stability of a bicontinuous geometry related to the I-WP surface in a hybrid mono-, poly-disperse terblock copolymer (monodisperse A-block, polydisperse B-block), discussed in Section 5.

The idea that packing frustration can be partially relieved by addition of homopolymer or by a polydisperse blend is not new. For example, the range of temperatures where the Gyroid is stable has been found to be increased by increasing the polydispersity in block copolymer systems [10]. Theorists have long argued that the cubic Diamond mesophase — that is more frustrated than the Gyroid mesophase — can be stabilised by addition of homopolymers [11] whose prime role is to relieve the frustration by filling the interstices that the polymer coils cannot reach without stretching. A similar explanation was proposed to account for the apparently more widespread occurrence of hyperbolic mesophases (including mesh and bicontinuous strut examples) in homopolymer-copolymer mixtures [12]. Addition of an inorganic component has been shown to give a mesophase based on the even more frustrated P(rimitive) minimal surface of symmetry $Im\overline{3}m$ [13] (we note that these authors explicitly ruled out that their structure might be based on the I-WP surface, which has the same space group as the P surface).

The influence of polydispersity of one or both moieties of a diblock copolymer on the self-assembly process has recently attracted renewed attention. A self-consistent field theory (SCFT) for diblock copolymers with strong polydispersity in one of the two blocks has been developed [14] and applied [15], though it has yet to be applied to complex hyperbolic geometries. Matsen has investigated polydispersity in strongly segregated block copolymers, also using SCFT [16]. Stepanow et al. have theoretically analysed symmetric AB diblocks with polydispersity, and conclude that polydispersity may result in the emergence of a glassy state [17]. Matsushita et al. have conducted experiments on symmetric copolymers with polydispersity in both blocks that resulted mostly in lamella structures [18]. Lynd and Hillmyer have experimentally analysed diblock copolymers with one monodisperse and one polydisperse block [15]. These studies confirm older theoretical predictions (from disordered systems) that the domain spacing (specifically in the lamellar phase) increases with increasing polydispersity [19,20]. Cooke and

Shi have studied symmetrically and asymmetrically polydisperse diblock copolymer systems using SCFT with a perturbation approach in the limit of small polydispersity [21]; the only bicontinuous structure included in their structure is the $Ia\overline{3}d$ double-Gyroid. Lynd and Hillmyer have also reported changes in the morphology of the phase as a consequence of changed polydispersity [15]. Our speculations here aim at such morphological changes. We hope that this article will motivate a fuller experimental and computational quest for alternative geometries that copolymers may adopt due to the effect of polydispersity.

The remainder of this article is organised as follows: Section 2 describes the point-wise definition of channel radius for arbitrary domains using the medial surface construction. Section 3 describes the model for the spatial structure of AB and linear ABC phases used here. It is based on parallel surfaces to triply-periodic minimal surfaces; these are not CMC surfaces. Section 4 describes the global geometry of the Gyroid surface in some detail, specifically discussing the widest and narrowest points of the channels. Section 5 contains the main result of this article that the I-WP surface may be a suitable candidate geometry for an alternating phase in an asymmetrically polydisperse polymer system. The appendix summarises useful formulae for the computation of curvature properties of the models analysed and provides additional geometric data on cubic bicontinuous surfaces.

2 Definition of point-wise domain widths (channel radii) via the medial surface construction

We provide a geometric definition of *local channel width* that is related to the linear span of individual polymer chains in the mesophase. We start with an arbitrary domain C, bounded by a surface S. Assume that S is sufficiently smooth and has a normal field N that points into the 'interior' of C. For every point p on S we define the *channel radius* $d(p)$ to be the greatest number such that p is (one of) the closest points on S to $q = p + d(p)\,N(p)$. The channel radius is a measure of the "width" or "depth" of C at the point p, as illustrated in Figure 1.

The structure one obtains by applying $p \to p + d(p)\,N(p)$ to all points p on S is called the *medial surface* [1,22–24]. Formally, the medial surface is the locus of all points in the domain C associated with more than one closest point on the bounding surface S; see e.g. points p and p' in Figure 1 with $ms(p) = ms(p') = q$. The MS is centred within the domain C, and correctly represents the topology and connectivity. The medial surface is similar to the older notion of the labyrinth graph, a 1D network that lines the channels of the structure, first used by Schoen to characterise triply-periodic minimal surfaces [25]. However, in contrast to the labyrinth graph, the medial surfaces encodes precisely the geometry of C [26]. The medial surface of a three-dimensional domain is in general composed of surface patches, and only degenerates to a one-dimensional graph if the cross-section of the domain is circular.

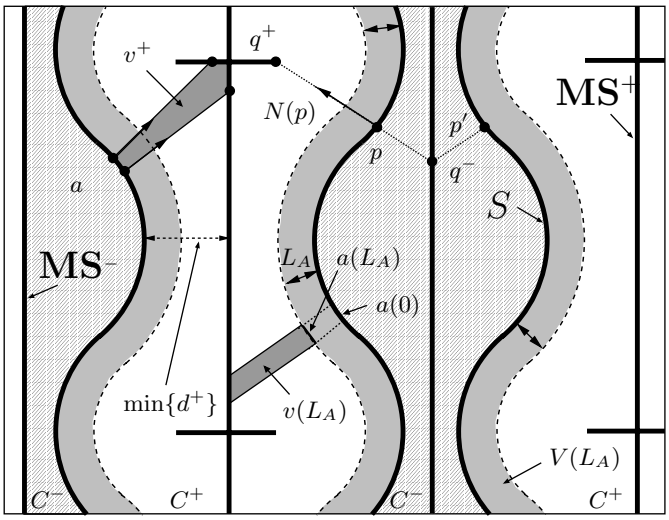

Fig. 1. Illustration of the medial surface (or axis, in 2D) construction: the surface S is the interface between two (distinct) domains C^+ (white and gray) and C^- (hashed), the two labyrinthine channels. The pair of medial surfaces on either side of the IMDS are labelled MS^+ and MS^-. The undulating grey slabs indicate parallel bodies of thickness L_A into the domain C^+. For every point p on S, there are corresponding points $q^\pm = ms^\pm(p) = p \pm d^\pm(p)\,N(p)$ on each of the two medial surfaces. A surface patch dA together with its associated volume element v^+ is also shown. The superscript $\pm$ indicates which labyrinth the volume cell is in; "+" if it is in positive normal direction, "−" otherwise. The volume elements extend from S to the MS in the corresponding labyrinth.

Figure 2 shows the medial surface structure of the Gyroid TPMS; it has the appearance of a twisted ribbon centred within the labyrinth channels. A detailed description of this structure for the Primitive, Diamond and Gyroid surfaces has been published elsewhere [1].

The medial surface concept provides a natural algorithm to construct elemental cell volumes associated with surface elements. This construction allows quantitative analysis of point-wise (hence *local*) volume-to-surface ratios in a structure whose global geometry is inhomogeneous. For a small area patch a, the corresponding volume element v^+ is the volume between a and its image on the MS in positive normal direction. Strictly speaking, it is the space foliated by parallel translation of a until the MS is reached, i.e. each point p of a is moved along its normal to $p + \min\{d(p), r\}\,N(p)$ with r ranging from 0 to $\max\{d(p)\}$. These prismatic volume cells are long and skinny for small surface patches a; their length is approximately given by the average MS distance function value $\langle d \rangle$ on a. The superscript $\pm$ indicates which labyrinth the volume cell is in; "+" if it is in positive normal direction, "−" otherwise.

We propose two measures of structural homogeneity; assuming that a given surface represents a free energy minimum for a copolymer system, these measures can then be related to the degree of chain packing frustration of the polymer chains. The first measure is the normalised width of the distribution of MS distance.

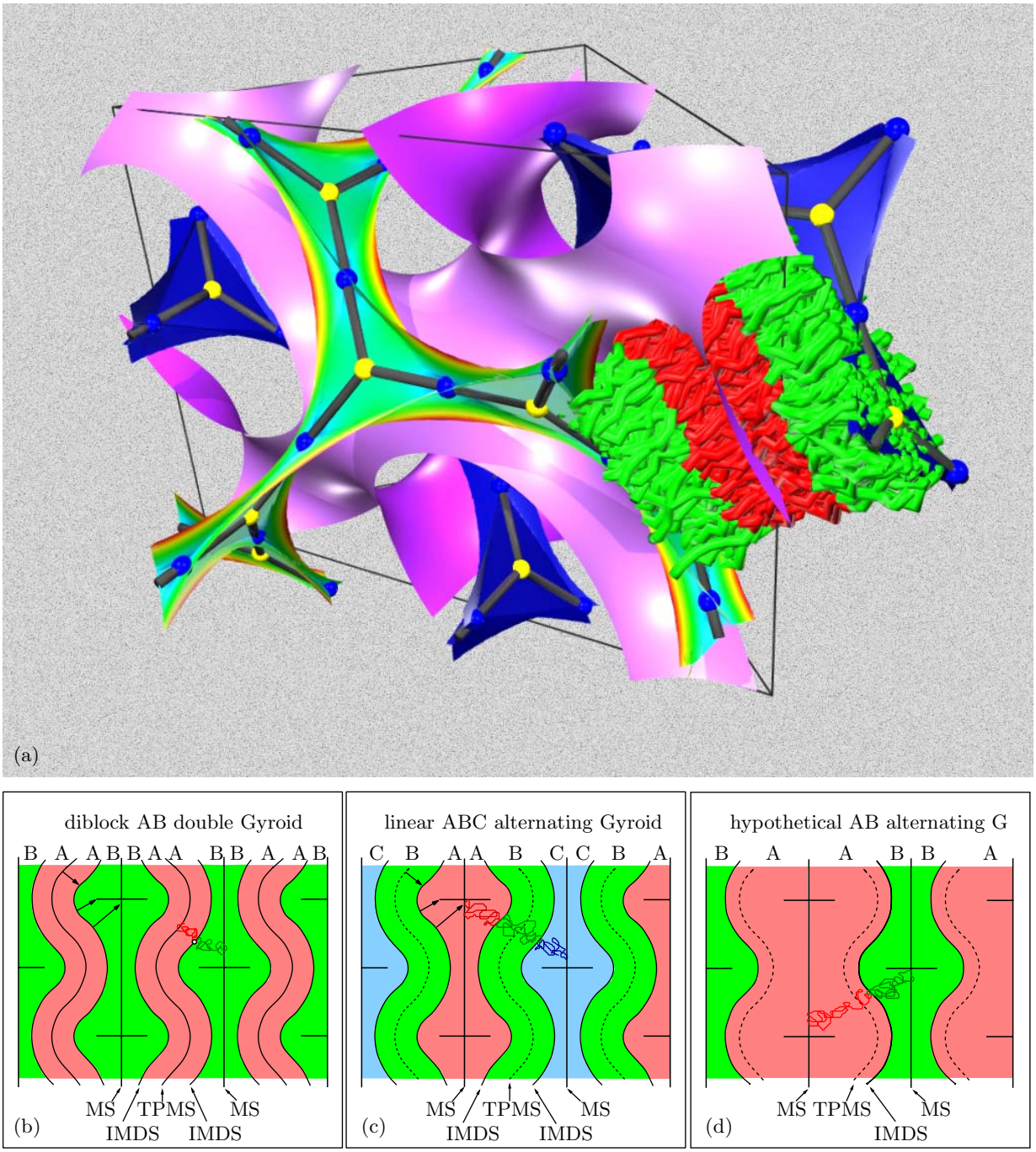

Fig. 2. The cubic Gyroid triply-periodic minimal surface and related copolymer mesophases: (a) The Gyroid is shown with its two congruent medial surfaces (MS), one coloured blue and the other coloured according to the value of the channel radius. Black edges indicate the three-coordinated labyrinth graphs in the MS, yellow spheres mark the graph nodes that coincide with the smallest channel radii of all points in the labyrinth graph (i.e. minima of d). Blue spheres mark the midpoints of labyrinth graph edges; these are the widest points of the channel domains. For better visibility, the Gyroid surface and the blue MS are clipped along the [110] plane. A schematic cartoon of the chains of AB diblock copolymers (red A, green B) in a double core-shell mesophase is also shown in a portion of the two labyrinths. The space available to each polymer extends from the Gyroid surface interface to the MS. (b–d) Illustrative 2D models for bicontinuous AB and linear ABC mesophases. Double- or Core-shell-Gyroid geometries have been identified in AB diblock and linear ABC copolymers. The alternating Gyroid geometry has also been found in linear ABC copolymers; for AB diblock copolymers this geometry has been shown not to be stable.

It is the most direct measure of thickness variation. In applying this measure to phase stability analysis, one assumes that the polymer block extends from the interface to the MS. This correspondence ignores the possibility of variations in area available for each molecule at the interface. The second measure allows for those variations and is defined as the normalised width of the distribution of local v/a ratios, with the volume cells of volume v and area a as defined above.

3 Model geometries for copolymer mesophases

This section describes the model geometry for core-shell and alternating bicontinuous phases used here. The IMDS are modelled as genuine parallel surfaces to triply-periodic minimal surfaces (TPMS) and do *not* have constant curvature. It is known from simulation and experiment that the IMDS in diblock copolymers deviates from these models; yet they represent a tractable approximation and have the advantage of being mathematically parametrised model surfaces with parameters that can be tuned easily.

TPMS are periodic and symmetric surfaces of vanishing mean curvature that divide space into two intertwined labyrinths [27]. The two labyrinths can be identical (as in the Diamond and Primitive surfaces [28]), chiral enantiomers (as in the cubic Gyroid surface [25]) or of different shape and volumes (as in the I-WP [25]). Figure 2a shows a fraction of the cubic Gyroid TPMS. We will occasionally refer to this Gyroid (i.e. with vanishing mean curvature) as *minimal Gyroid* to distinguish it from surfaces with the same symmetry or topology (such as parallel surfaces to the minimal Gyroid, or other models for the IMDS) that are also often called Gyroid.

In the model for the double- or core-shell-geometries (illustrated in Fig. 2) used here, the IMDS between the A and B blocks is given by two parallel surfaces $S_{1/2}$ at distance L_A from the corresponding TPMS, i.e. $p \to p \pm L_A\, N(p)$ for any point on the TPMS. Therefore the length L_A corresponds to half the thickness of the A phase. The TPMS itself lies in the A domains, lining its mid-surface and defining the hypothetical A-A interfaces of molecular ends. The A domain is the volume between these two parallel surfaces, whereas the B domain naturally separates into two intertwined networks. Both the mean and Gaussian curvature of the IMDS $S_{1/2}$ are not constant; the domain A is of constant thickness $2L_A$ whereas the B domain has varying width. See Figures 2b and 2a.

We restrict the parallel distance L_A to be smaller than the minimal MS distance, $L_A < \min\{d(p)|p \in S\} =: d_0$. Without this restriction, the parallel surfaces would develop cusps and the parallel foliation would multiply tile the volume. It is clear from Figure 8 in Appendix, which shows data for $r < d_0$ only, that this restriction is fulfilled for all reasonable volume ratios.

For the alternating phase of linear ABC copolymers (Fig. 2c), we again make the assumption that the two IMDS (separating A and B domains, and B and C domains) are parallel surfaces to the underlying TPMS. Assuming reasonable volume ratios of the three components, one IMDS is offset from the TPMS by a positive distance d_{AB} and the other by a negative distance $-d_{BC}$; their absolute values are not generally the same, see Figure 2c. In this model geometry, the domain of component B is of constant thickness, whereas the dimensions of A and C vary. Finally, the AB alternating geometry (Fig. 2) — that has never been observed in copolymer blends — contains only one IMDS that is parallel to the TPMS, see Figure 2d.

Due to the unavoidable fluctuations of the Gaussian curvature K on minimal surfaces (for which $H = 0$), any parallel surface to a TPMS has (by virtue of Eq. (3)) fluctuations of the mean curvature. However, in particular for the hypothetical alternating AB phase with comparable block volumes, these models are approximations to CMC surfaces with small deviations. The deviations from constant curvature are quantified in Figure 8 in Appendix. The advantages of our parallel surface models outweigh their possible inaccuracies. They provide the most concise geometric data possible; their average curvatures and channel diameters, and variations thereof, are given by simple analytical functions, see appendix.

Depictions of such partitions are found throughout the copolymer [13], liquid crystal [29] and TPMS [30] literature. An explicit comparison of the parallel to the CMC geometries is possible and desirable.

To avoid confusion in the remainder of this article we clarify the notation for the various phases: The standard $Ia\overline{3}d$ Gyroid phase, also called *double-Gyroid*, and the *core-shell* $Ia\overline{3}d$ Gyroid phase in linear ABC triblock terpolymers are phases where both of the two intertwined, geometrically congruent network domains are chemically identical and each contain *all* components of the copolymer, see Figure 2a. Hence, the symmetry group $Ia\overline{3}d$ contains elements that exchange the two labyrinths (specifically this is a $\overline{3}$ inversion on the surface). The terms *core-shell Gyroid* and *double-Gyroid* mean, from a geometric perspective, the same structure, one term being used for ABC terpolymers, the other for AB diblock copolymers. In contrast, the *alternating Gyroid phase* in linear ABC terpolymers has symmetry $I4_132$ that does *not* contain elements exchanging the two sub-domains. This reflects the fact that one domain is composed of moiety A, and the other of moiety B with a matrix of C, that is folded onto the minimal Gyroid surface, separating them. The mathematical minimal Gyroid surface, as parametrised by the Weierstrass equations or the approximation given in equation (1), is the structural basis for both. It can be embedded in both symmetry groups, depending whether it is oriented (i.e. with surface normals, $I4_132$) or not ($Ia\overline{3}d$). The *alternating I-WP phase* that is postulated in Section 6 is also one with two chemically distinct domains. The space group $Im\overline{3}m$ does not contain symmetry operations exchanging the two labyrinthine domains. We note that a double- or core-shell-phase based on the I-WP is actually impossible as the two domains are geometrically distinct.

4 Domain widths in the Gyroid phase

In the simpler Primitive and Diamond TPMS, the nodes of the line graph (LG) define the largest voids of the labyrinthine domain [1]. For the minimal Gyroid the opposite is true: the nodes of the LG define centres of the smallest voids, the widest voids, corresponding to the maximal radii of the Gyroid channels, are located at the centres of the LG edges. This has been demonstrated for the exact minimal surface Gyroid geometry parametrised by the Weierstrass equations [1]. These parametrise the Gyroid TPMS via path-integrals in the complex double-sheeted complex plane, see e.g. [31]. Here we present calculations that show that it also holds true for the nodal Gyroid surface, which gives an interface slightly different from the TPMS and is often used as an approximation for the minimal Gyroid. The nodal Gyroid is given by the following implicit equation for its surface points [32,33]:

$$\cos(2\pi x)\sin(2\pi y) + \cos(2\pi y)\sin(2\pi z) + \cos(2\pi z)\sin(2\pi x) = 0. \quad (1)$$

The differences between these two representations are small and the observations of this article hold true for both nodal and Weierstrass representations.

Figure 2a shows a portion of the cubic Gyroid surface, in purple, together with the MS in both labyrinths and LGs with yellow and blue spheres marking the LG nodes and the edge midpoints, respectively. One of the two MS is coloured in blue, the other according to a colour scheme that indicates the point-wise defined channel diameter (as measured by the MS distance function); the channel diameter increases in the order red, yellow, green, blue. The Gyroid surface is computed from the nodal representation, equation (1), and the MS is computed using the algorithm described in [4].

We consider one of the (identical) labyrinths bounded by the Gyroid surface and define the local channel radius by the MS distance function $d(q)$ from a point q on the MS to (one of) the nearest point p on the Gyroid surface (with $q = ms(p)$). The important observation is that the three-coordinated LG nodes (yellow spheres) have a local channel diameter that is 5.9% smaller than the channel diameter at the LG edge midpoints (blue spheres). We note that the differences between the nodal and Weierstrass Gyroid representations are so small that this number is the same for both.

For the domain geometries described in Section 3, i.e. bounded by a parallel surface at distance L_A to the Gyroid TPMS, this result remains valid. The local thickness of the labyrinth is then given by $d(p) - L_A$ (as the IMDS is chosen as a true parallel surface at constant distance L_A from the TPMS). The ratio between the channel diameter at the edge midpoint to that at the 3-node is given by $(d_{max} - d_{min})/(d_{min} - L_A)$, i.e. it increases with increasing L_A (see Tab. 1 in Appendix).

This result is obtained for the minimal Gyroid interface ($H = 0$) and for parallel surfaces to the Gyroid TPMS. Its validity for the family of CMC Gyroid surfaces [34] needs to be assessed. However, that family contains the minimal Gyroid as the family member with $H = 0$. In that limit the edge midpoints are the widest points. For the members with high mean curvature (or low volume fraction of the minority component) the nodes clearly are the widest points, see Figure 5 in [34]. Hence, for the CMC Gyroid family there is a volume fraction (or curvature) where the widest point of the labyrinth moves from the edge midpoint to the channel graph vertex.

It is worth noting that the points p_n on the TPMS that correspond to the LG node q_n, i.e. $ms(p_n) = q_n$, are flat points of the surface, i.e. of vanishing Gaussian curvature $K(p_n) = 0$. This holds true for the cubic Gyroid, Primitive and Diamond surfaces [1]. This implies that the volume cell corresponding to an infinitesimal area element at the flat point does not shrink in width with increasing parallel distance from the TPMS, see equation (6). For the Diamond and Primitive surfaces where the LG nodes are the widest labyrinth points, i.e. with maximal $d(p_n)$, the widest volume elements are also the longest, hence with largest v/a (assuming equal area a). For the cubic Gyroid TPMS the widest volume cells at the flat points are *not* the longest, which balances that effect. This affects the distributions of local v/a ratios, discussed in Section 5.

5 Domain widths and v/a distributions of the cubic I-WP, Gyroid, D and P surfaces

The I-WP surface, named by Alan Schoen, is of cubic symmetry $Im\overline{3}m$ [25,35]. Its two labyrinthine subdomains are not congruent. One labyrinth is termed I, referring to the body-centred LG representation (*innen-zentriert*), the other is the WP (or *wrapped parcel*) labyrinth, named after the pattern of edges in a unitcell of the WP labyrinth graph, that resembles the tying of a string around a parcel [25]. We have determined that the I labyrinth encloses a total volume fraction of 0.536, in agreement with [36]. (Note that the simpler P, D and Gyroid TPMS are *balanced*, i.e. partition space into two equal volumes.) We shall see that the two labyrinths of the I-WP geometry have very different channel radii distributions; the I labyrinth has thickness variations larger than the cubic Primitive surface, whereas the variations of the WP labyrinth are of similar magnitude to the cubic Gyroid.

The geometry of the I-WP surface and its two MSs is shown in Figure 3 (top). With respect to the conventional location and size of the cubic body-centred translational unitcell in the $Im\overline{3}m$ space group (which is twice the primitive translational unitcell), the I labyrinth contains large pores at the body-center and at the eight corners of the cube and channels along the body-diagonals connecting these pores (Note that the I-WP has the same symmetry as the cubic Primitive surface, but with a distinct geometry. In fact, for the I-WP this symmetry group does, of course, not contain any operations exchanging the two domains, whereas it does for the Primitive surface). In contrast to the Gyroid case, the nodes of the I LG define centres of maximal channel width d_{max} and the edge mid-points mark the narrowest, nearly circular, constrictions of distance d_{min}. The ratio of the channel radii is $d_{max}/d_{min} \approx 2.1$.

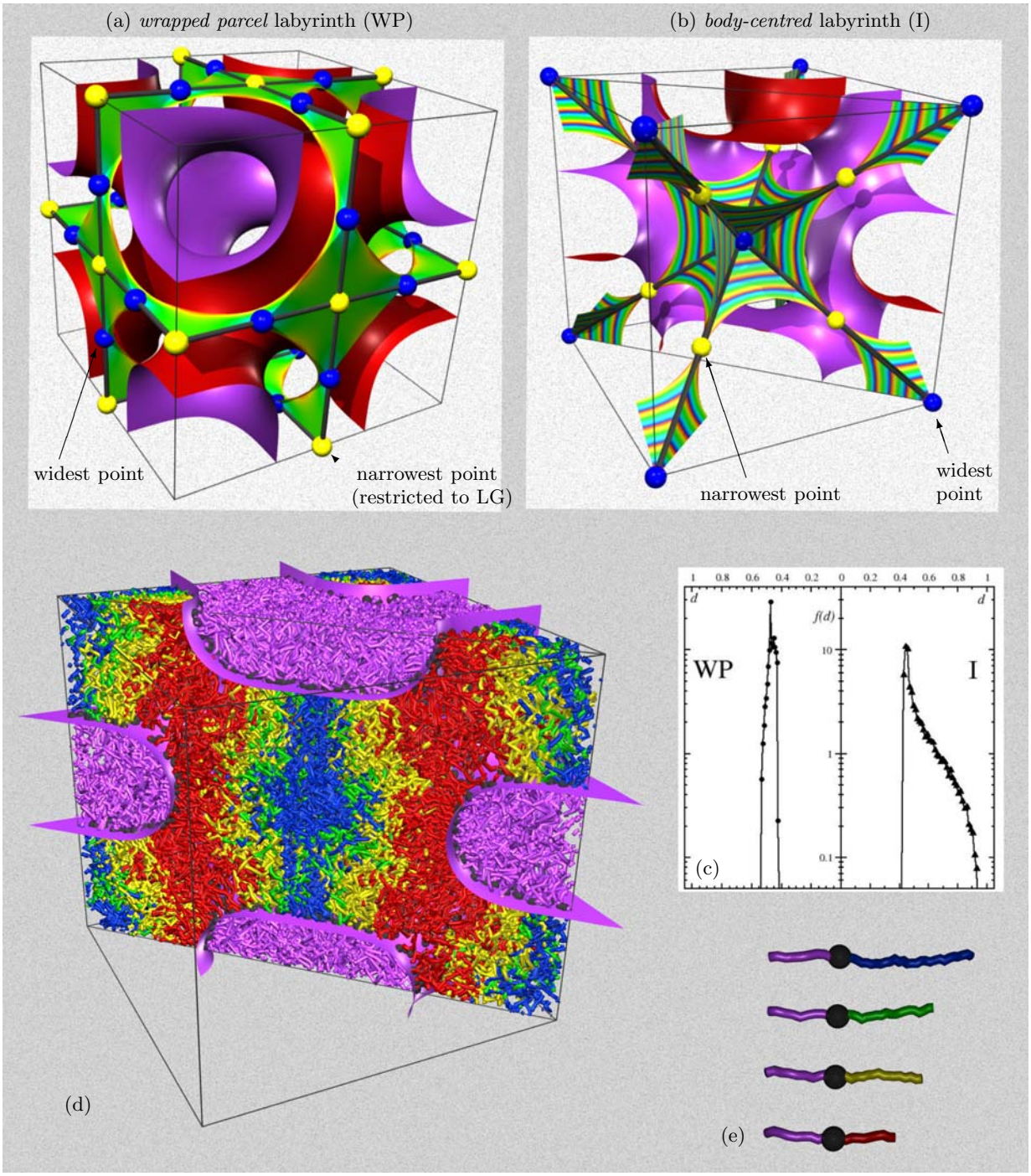

Fig. 3. The I-WP surface in the context of block-copolymer self-assembly: (top) the I-WP partitions space into two intertwined but geometrically different labyrinths, I and WP, of distinctly different properties. A conventional cubic translational unitcell of the I-WP surface is shown, coloured red on the WP and purple on the I side; in (b) the surface is clipped along a vertical plane containing a face diagonal, for better visibility. The two medial surfaces in the WP and I labyrinths are also illustrated. The colouring indicates contours of the distance function, with the same contour differences in (a) and (b). Blue spheres indicate maxima of the distance function $d(p)$; yellow spheres indicate minima of $d(p)$ *along* the line graphs. (c) Distribution of MS distance functions for the WP and I labyrinths. (d and e) For a linear ABC terpolymer blend with monodisperse A and B component (purple) and with a polydisperse C component that approximately conforms to the distribution of $d(p)$ for the I labyrinth, a stable alternating I-WP phase of symmetry $Pm3m$ is suggested.

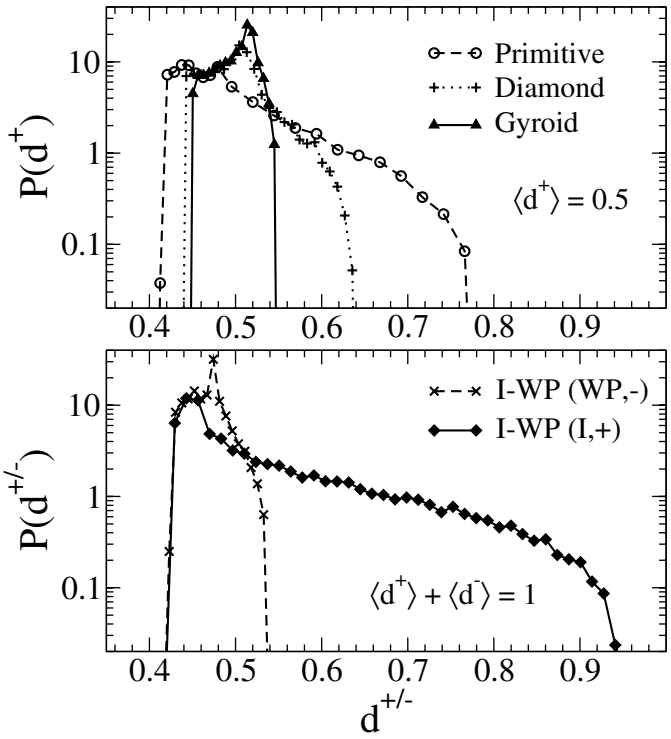

Fig. 4. Distributions of channel radii $d(p)$ for the cubic minimal Primitive, Diamond, Gyroid, and the two sides of the I-WP surfaces. The length scale of the surfaces is set such that the average channel radius is $\langle d^+\rangle + \langle d^-\rangle = 1$. All $d(p)$ values with finite probability are shown in the diagrams. Note that these distributions, as well as the ones in Figure 5, are area-weighted, i.e. $P(d') = 1/A \int_S da(p)\, \delta(d' - d(p))$.

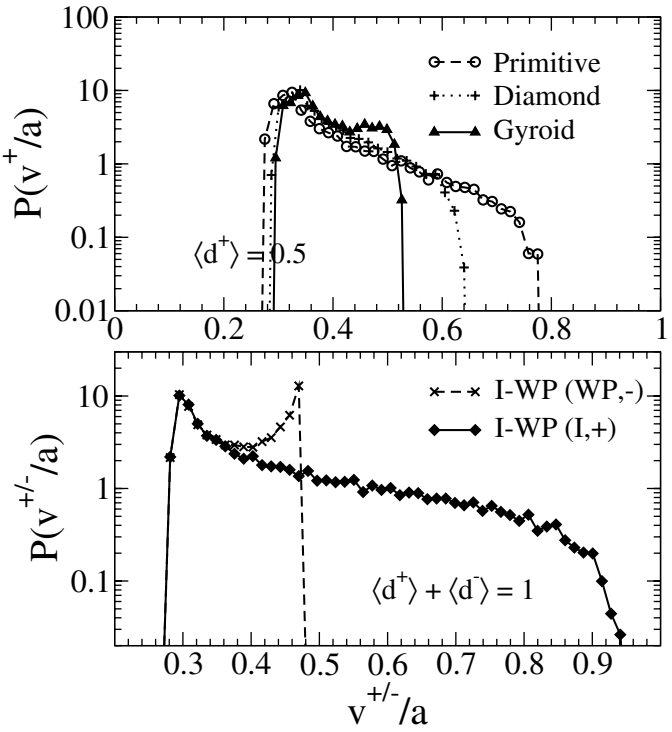

Fig. 5. Distributions of point-wise v^+/a ratios for the cubic minimal Primitive, Diamond, Gyroid, and the two sides of the I-WP surfaces. The length scale of the surfaces is set such that the average channel radius is $\langle d^+\rangle + \langle d^-\rangle = 1$. All v^+/a values with finite probability are shown in the diagrams. See also the notes in appendix 7 on the extremal v/a ratios.

The MS geometry of the I labyrinth resembles that of the Primitive surface [1], containing planar "sails" that span pairs of the LG edges emanating from the LG nodes. The body-diagonals define branch lines of the MS, along which three such sails meet. At the LG edge midpoints the MS shrinks almost to a line, due to the quasi-circularity of the constriction. We note the discussion of the I-WP surface in the context of smectic liquid-crystal phases in references [37,38]

The WP labyrinth in this surface is geometrically very different. The WP LG contains *planar* nodes of degree four (located at sites with point group symmetry $4/mm.m$). The nodes, with d_{min}, are the narrowest points along the LG, whereas the edge midpoints (at $\overline{4}m.2$) are the widest points of the labyrinth, with d_{max}. In this labyrinth the ratio d_{max}/d_{min} is 1.1. The MS consists mostly of planar square patches that merge pairwise at the LG edge midpoints. This pattern compares with that of the Gyroid MS, where the MS consists of triangular patches.

The local channel radius of the I labyrinth has very large fluctuations, whereas the WP labyrinth is rather uniform in dimension, comparable to the cubic Gyroid. Figure 4 shows the distribution of the MS distance function, i.e. the local channel radii, for the I and the WP labyrinth. The data shown is for lattice parameter $l_{Im\overline{3}m}$ such that $\langle d^+\rangle + \langle d^-\rangle = 1$, see Table 1. Without a theory that fixes the length scale, this normalisation has to be considered a heuristic choice. Alternatively, a constant $\langle v/a\rangle$ ratio could have been chosen. We emphasise that the results of this article hold for both of these normalisations. The data for the cubic Gyroid, Diamond and Primitive surfaces are shown for comparison demonstrating that the Gyroid is the least packing frustrated surface among these three. The distribution of local v/a ratios corroborates this claim, see Figure 5. Again, the WP channel distribution has similar width to the Gyroid, whereas the distribution of the I channel is wider than the distribution of the Primitive surface.

These data are applicable immediately to the case where the IMDS coincides with the TPMS, i.e. for example for a hypothetical alternating AB phase with equal block volumes for the Gyroid, or almost equal block-volumes $v_1 = 0.467$ and $v_2 = 0.533$ for the I-WP surface. In general, the IMDS is not identical to the TPMS but is rather (modelled as) a parallel interface to the TPMS with distance L_A, e.g. for the usual core-shell Gyroid phase. For the general case, the volume cells $v(L_A)$ extend from the parallel surface of the TPMS at distance $r = L_A$ to the MS. The area patch $a(L_A)$ is on the IMDS, i.e. on the parallel surface to the TPMS. We characterise the distributions of $v(L_A)/a(L_A)$ for a given L_A by their standard

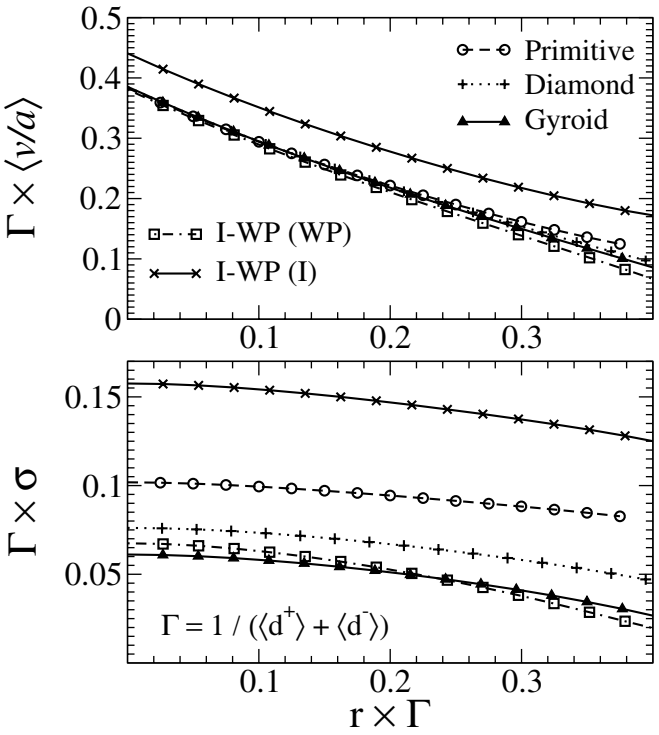

Fig. 6. Average (global) v/a ratio and its fluctuations $\sigma = \sqrt{\langle (v/a - \langle v/a \rangle)^2 \rangle}$ for the parallel surface at distance r, i.e. the volume cells extend from surface patches on the parallel surface to the medial surface (such as the minority component in an AB core-shell Gyroid). Data is presented for the Gyroid, Diamond, Primitive and the two channels of the I-WP surface. The factor $\Gamma = 1/(\langle d^+ \rangle + \langle d^- \rangle)$ rescales the data such that, on average, the average channel radius of each labyrinth of the TPMS ($r = 0$) is 0.5, i.e. $\langle d^+ \rangle + \langle d^- \rangle = 1$.

deviation, $\sigma = \sqrt{\langle (v/a - \langle v/a \rangle)^2 \rangle}$ (see Appendix for the relation between the relative block volumes and L_A). Figure 6 shows the variations of the $v(r)/a(r)$ ratios for parallel surfaces at distance r. Correspondingly, averages are weighted by the area of the parallel surface area patches $a(r)$ and not $a(0)$. See also Figure 1 for an illustration of these volume cells.

6 Speculation on Im$\bar{3}$m (I-WP) mesophases in asymmetrically polydisperse copolymers

The very high global packing homogeneity of the WP labyrinth — comparable to the Gyroid case — points to the possible occurrence of the I-WP geometry in copolymer mesophases, provided the relatively inhomogeneous I labyrinth can be accommodated by suitable polymeric blocks. We therefore suggest that a blend of AB (or linear ABC) block-copolymers, with monodisperse blocks A (or A and B) coupled to adjacent blocks C whose molecular weight polydispersity is higher, may self-assemble into an "alternating I-WP" mesophase. The idea, illustrated in Figure 3, is that the polydispersity will allow molecular segregation such that copolymers with larger blocks will be located to fill the wider regions in the I labyrinth, whereas the smaller copolymer species will reside in narrower regions.

The polydispersity data presented so far, i.e. the standard deviation of the distribution of channel radii $d(p)$, can be approximately transformed into the more conventional measure used by polymer chemists, the polydispersity index (PDI). The PDI is defined as the weight-average molecular weight divided by the number average molecular weight. In a geometric sense, the variations of $d(p)$ relate to the PDI of a molecular assembly that is assumed to adopt the given surface as the free energy minima. One assumes that the end-to-end distance L corresponds to the MS distance function $d(p)$, that the relation between the degree of polymerisation M and L follows the power law $L \propto M^{2/3}$ [39] and that the polydispersity matches the distribution of $d(p)$. Figure 7 shows the PDI of the polydisperse block C as a function of its volume fraction (for the hypothetical alternating AB phase, the nearly monodisperse phase consists of the A blocks, and for the alternating ABC phase of the combination of A and B blocks. IMDS here always denotes the interface between the polydisperse and the nearly monodisperse phase). In particular for the case where the IMDS is identical to the I-WP TPMS, the PDI values are (1.12 ± 0.01) for the C blocks and (1.00 ± 0.01) for the nearly monodisperse phase. Systems with such parameters are known to adopt lamellar geometries [15], hence an I-WP AB alternating phase with $f_C = 0.53$ is unlikely. In the presented approximations, the PDI for the cubic Gyroid evaluates to (1.00 ± 0.01), yet the Gyroid is frequently found at larger PDIs [15]. Nevertheless, the data presented in Figure 7 should represent a starting point for experimental verification of our speculation about the existence of an I-WP phase in asymmetrically polydisperse polymer blends. In particular, if the volume fraction f_C of the polydisperse component is smaller than that of the monodisperse component, the PDI of the polydisperse component rises strongly. It is in this regime rather than the lamellar-forming regime, where we anticipate finding the alternating AB diblock I-WP $Im\bar{3}m$ phase.

The arguments presented so far also apply to a linear ABC terpolymer with monodisperse A and B components and a polydisperse C moiety. In fact, linear ABC terpolymers may offer a better starting point for the search for this phase, as an *alternating* Gyroid phase exists for these systems. We suggest that the experimental search for this mesophase should proceed from a monodisperse system in an alternating $I4_132$ Gyroid phase (e.g. [40]) by a gradual increase in the PDI of moiety C while keeping A and B as monodisperse as possible.

Our suggestion is based on a model with the following implicit assumptions: (1) the IMDS is described by a parallel surface to a minimal TPMS, and is hence not a CMC surface. See Figure 8 for a quantification of the deviations from constant mean curvature. (2) The interface between the different components of the polymer is sharp and can be described by a two-dimensional IMDS. (3) The orientation of the blocks is perpendicular to the IMDS.

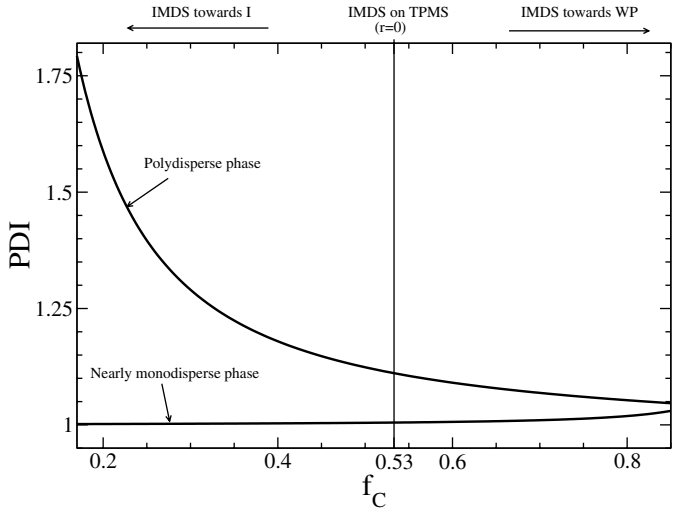

Fig. 7. The polydispersity index as function of the volume fraction f_C of the polydisperse phase C. For details see text.

(4) Packing frustration of the chains can be related to variations of the local channel thickness or to local volume-to-surface measures relative to the statistical length of the polymer chains. In real polymer systems, there are deviations from these assumptions. Nevertheless, we trust them to be sufficiently accurate for our hypothesis to be qualitatively valid for experimental copolymer systems.

We comment on previous experimental work: Lynd and Hillmyer have analysed a diblock system with similar values of the PDI as suggested here [15]. They show that for $f_C = 0.5 \pm 0.1$ the lamellar phase persists even when asymmetric polydispersity is present, e.g. $\mathrm{PDI}_A = 1.2, \mathrm{PDI}_C \leq 2.0$. However, in the regime where we expect the influence of PD to be evident they observe a morphological transition to the Gyroid when varying PDI_C. So their results do not falsify our hypothesis regarding the I-WP phase in AB diblock copolymers.

7 Conclusions

Our analysis of various bicontinuous morphologies is based on the concept of a medial surface. For a given labyrinth the medial surface (MS) is a two-dimensional skeleton centred within the labyrinthine domain. The point-wise distance between a point on the labyrinth surface and the corresponding point on the MS provides a robust definition of local channel diameter. This construction improves earlier definitions, that defined this distance to be equal to the separation between the interface and the 1D labyrinth graph, or that were based on planar cross-sections. The latter assumption is too crude to tease out differences between bicontinuous structures in detail. The former is mathematically ill-defined, since a 1D graph cannot encode the geometry of the 2D interface. The analysis quantifies the notion of global packing frustration in bicontinuous block-copolymer mesophases that results from stretching of the polymer coils in order to fill space uniformly.

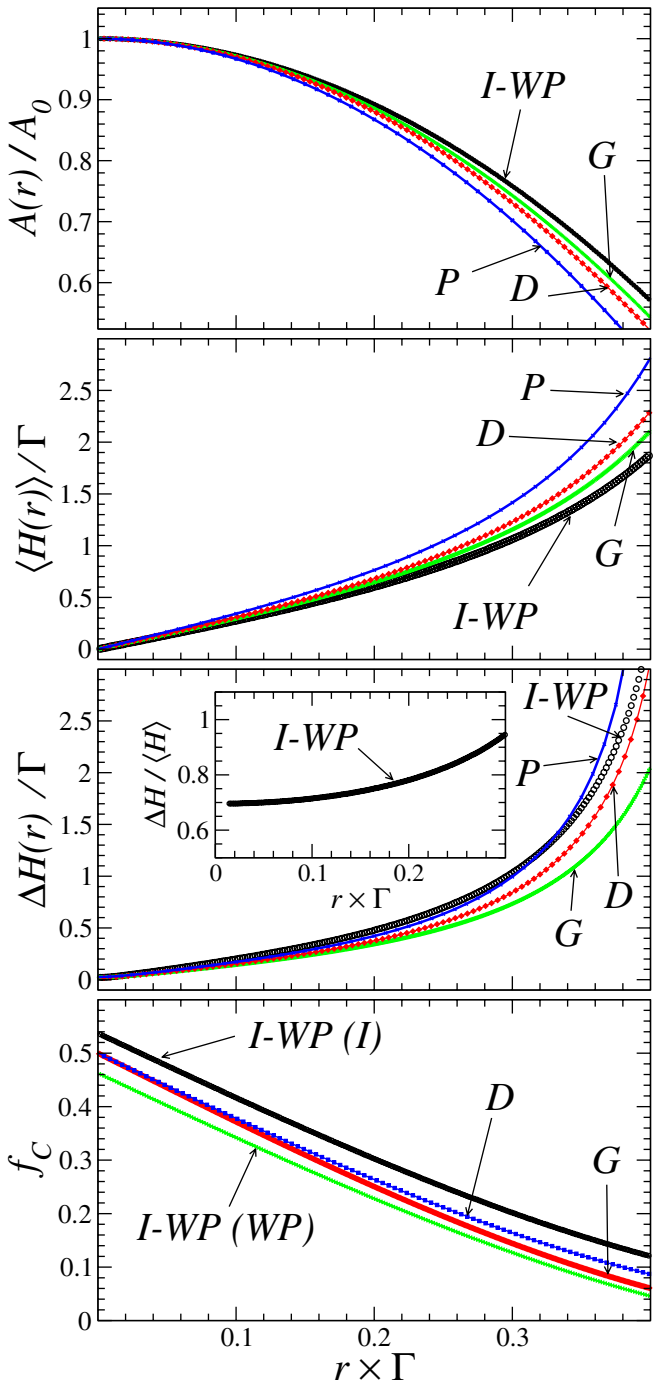

Fig. 8. Area, volume, average and standard deviation of mean curvature of the parallel surfaces to the I-WP, Gyroid, Diamond and Primitive surfaces as a function of parallel surface distance r. The constant $\Gamma = 1/(\langle d^+ \rangle + \langle d^- \rangle)$ normalises these data to $\langle d^+ \rangle + \langle d^- \rangle = 1$, i.e. average channel radius is 0.5. See text for details. Note that this data is valid for true parallel surfaces, i.e. $r < \min\{d(p) | p \in S\}$ holds for all r shown here. The volume fraction $f_C(r)$ is defined as $f_C(r) = [V^- + V(r)]/(V^- + V^+)$ where $V(r)$ is the volume of the parallel body, V^+ the volume of the second labyrinth (i.e. in negative r direction from the surface) and $V^+ = V(r \to \infty)$ the volume of the labyrinth that is foliated by the parallel body. See also Table 1 for definition and values of the constants used here.

We have applied this definition to the cubic Gyroid triply-periodic minimal surface, and have shown that the three-valent nodes of the channel graph are actually the narrowest points along this graph, whereas the edge midpoints are the widest points of the labyrinth. This result is obtained for the Gyroid minimal surface geometry as well as its related nodal surface representation, or parallel interfaces thereof (it does not necessarily apply to the CMC Gyroid family of [34], although holds in the vicinity of the member with vanishing mean curvature).

Geometric analysis of channel radii (as measured by the medial surface) and of local v/a ratios of the cubic Gyroid and I-WP triply-periodic minimal surfaces reveals similarities between these morphologies, particularly between the WP labyrinth of the I-WP surface and the Gyroid labyrinths. We hypothesise the I-WP might be a stable *alternating* equilibrium structure, with 3D symmetry $Im\overline{3}m$, for a linear ABC terpolymer with monodisperse AB blocks and polydisperse C block, or possibly even for a linear diblock copolymer system (AB) with strong polydispersity in the degree of polymerisation of one block and a relatively monodisperse distribution in the other block. The polydispersity of the polymers is accommodated by the variations of the labyrinth thickness, to relieve packing frustration that would otherwise prevent this phase from forming. We note that polymer blends with controlled polydispersity of one of the two components can be produced [15,41] and that our prediction can be verified numerically by modern SCFT methods [14].

STH acknowledges support from the Australian Research Council through a Federation Fellowship. GEST acknowledges support from the Deutsche Forschungsgemeinschaft through grant SCHR 1148/2-1.

Appendix: Curvature calculations

The model calculations presented in this article rely on Weierstrass representations of the underlying minimal surfaces. These are integral formulae for the three coordinates as path integrals in the complex plane; their numerical integration yield estimates for the point coordinates and their Gaussian curvature to any desired accuracy. The Weierstrass formulae for P, D, G and I-WP surfaces are well-known, see discussions in [31]. This appendix briefly reviews the calculation of Gaussian and mean curvature of parallel surfaces to these minimal surfaces.

Consider a regular surface $\mathcal{S}$ with point-wise defined Gaussian and mean curvature $K(p)$ and $H(p)$ and point normal $N(p)$ with $|N(p)| = 1$ for any point $p \in \mathcal{S}$. The surface $\mathcal{S}'$ is a parallel surface to $\mathcal{S}$ at distance r that is also assumed to be regular. (Regularity is a differentiability requirement for surfaces; see [42] for a proper definition. For our discussion, it suffices to say that the minimal TPMS and their parallel surfaces at distance r with $0 \le r < \min\{d(p)|p \in \mathcal{S}\}$ are regular.) Any point $p' \in \mathcal{S}'$ is related to a point $p \in \mathcal{S}$ by $p' = p + r\,N(p)$.

The Gaussian and mean curvature of $\mathcal{S}'$ at a point p' on $\mathcal{S}'$ can be expressed in terms of the Gaussian and mean curvature of $\mathcal{S}$ at point p through the following two formulae:

$$K(p') = \frac{K(p)}{1 - 2r\,H(p) + r^2\,K(p)} = \frac{K(p)}{1 + r^2\,K(p)} \qquad (2)$$

$$H(p') = \frac{H(p) - r\,K(p)}{1 - 2r\,H(p) + r^2\,K(p)}) = \frac{-r\,K(p)}{1 + r^2\,K(p)} \qquad (3)$$

where the rightmost terms are valid for a parallel surface to a minimal surface, i.e. $H(p) = 0$ for all points on $\mathcal{S}$.

Of interest are also the integrated curvatures $\mathcal{H} = \int_S H$ and $\mathcal{K} = \int_S K$, the area $A(r)$ of the parallel surface, and the volume $V(r)$ between the original surface and the parallel surface at distance r. These are known as Minkowski integrals in integral geometry [43]. The Minkowski integrals of a parallel surface can be expressed by simple polynomials in r, with coefficients given by the Minkowski integrals of the original surface (with subscript 0) [43]:

$$\mathcal{K}(r) = \mathcal{K}_0 \qquad (4)$$

$$\mathcal{H}(r) = \mathcal{H}_0 - \mathcal{K}_0\,r \qquad (5)$$

$$A(r) = A_0 - 2\mathcal{H}_0\,r + \mathcal{K}_0\,r^2 \qquad (6)$$

$$V(r) = A_0\,r - \mathcal{H}_0\,r^2 + \frac{\mathcal{K}_0}{3}\,r^3. \qquad (7)$$

The parameters A_0, $\mathcal{H}_0$ and $\mathcal{K}_0$ for the minimal TPMS are summarised in Table 1. The length scale of the structures (which is not set by the minimality condition) is chosen such that the average channel diameters add up to 1, $\langle d^+\rangle + \langle d^-\rangle = 1$. Figure 8 shows $K(r)$, $H(r)$, $A(r)$ and $V(r)$ for the P, D, G and I-WP surfaces. Note that in the regime shown here, i.e. $0 \le r < \min\{d(p)|p \in \mathcal{S}\}$, these functions are determined by curvature alone; they are identical for both sides of the labyrinths, even for the I-WP surface.

Table 1. Characteristics of the I-WP, Gyroid, Diamond and Primitive surfaces. The cell parameter a_s is chosen such that $\langle d^+\rangle + \langle d^-\rangle = 1$. For the I-WP surface the superscript '+' refers to WP, and '−' to I. $V_0 := V^+ + V^-$ is the total volume (on both sides) associated with the asymmetric unitpatch.

	I-WP	Gyroid	Diamond	Primitive
Non-oriented sym. group	$Im\overline{3}m$	$I4_132$	$Fd\overline{3}m$	$Pm\overline{3}m$
a_s	2.8456	2.3825	2.9563	1.7968
A_0	0.2922	0.3657	0.1747	0.1580
V_0	0.2400	0.2818	0.1346	0.1211
V^+	0.1111	$= V/2$	$= V/2$	$= V/2$
V^-	0.1290	$= V/2$	$= V/2$	$= V/2$
$\langle d^+\rangle$	0.4670	1/2	1/2	1/2
$\langle d^-\rangle$	0.5330	1/2	1/2	1/2
$\langle K_0\rangle$	−2.6882	−2.8637	−2.9969	−3.3139
ΔK_0	1.8701	1.3367	1.4057	1.5511
V/A	0.8213	0.7705	0.7701	0.7667
d_0	0.42	0.4485	0.4384	0.4166

For interfaces based on minimal surfaces or parallel surfaces to minimal surfaces, one can draw two interesting conclusions. Firstly, for a TPMS patch dA at point p (small enough so that we can assume the curvature is constant on it) equations (6) and (7) imply that v/a cannot be greater than $d(p)$. Second for points p on a TPMS where $d(p)$ corresponds to the radius of curvature, hence $K(p) = 1/(d(p))^2$, it follows that $V/A = 2/3\, d(p)$. This is for example the case for the points with minimal distances on the Primitive, Diamond, Gyroid and both sides of the I-WP surfaces, and agrees with the smallest v/a values with finite probability in Figure 5.

References

1. G. Schröder, S. Ramsden, A. Christy, S. Hyde, Eur. Phys. J. B **35**, 551 (2003)
2. M.W. Matsen, M. Schick, Phys. Rev. Lett. **72**, 2660 (1994)
3. M. Matsen, F. Bates, Macromolecules **29**, 1091 (1996)
4. G. Schröder-Turk, A. Fogden, S. Hyde, Eur. Phys. J. B **54**, 509 (2006)
5. M. Matsen, F. Bates, Macromolecules **29**, 7641 (1996)
6. H. Jinnai, Y. Nishikawa, R. Spontak, S. Smith, D. Agard, T. Hashimoto, Phys. Rev. Lett. **84**, 518 (2000)
7. P. Olmsted, M. Milner, Macromolecules **31**, 4011 (1998)
8. P. Duesing, R. Templer, J. Seddon, Langmuir **13**, 351 (1997)
9. M. Matsen, F. Bates, J. Chem. Phys. **106**, 2436 (1997)
10. F. Martínez-Veracoechea, F. Escobedo, Macromolecules **38**, 8522 (2005)
11. M. Matsen, Phys. Rev. Lett. **74**, 4225 (1995)
12. H. Hasegawa, T. Hashimoto, S. Hyde, Polymer **37**, 3825 (1997)
13. A. Finnefrock, R. Ulrich, G. Toomes, S. Gruner, U. Wiesner, J. Am. Chem. Soc. **125**, 13084 (2003)
14. S. Sides, G. Fredrickson, J. Chem. Phys. **121**, 4974 (2004)
15. A. Lynd, M. Hillmyer, Macromolecules **38**, 8803 (2005)
16. M. Matsen, Eur. Phys. J. E, Eur. Phys. J. E **21**, 199-207 (2006)
17. S. Stepanow, A. Dobrynin, T. Vilgis, K. Binder, J. Phys. I France **6**, 837 (1996)
18. Y. Matsushita, A. Noro, M. Iinuma, J. Suzuki, H. Ohtani, A. Takano, Macromolecules **36**, 8074 (2003)
19. K. Hong, J. Noolandi, Polym. Commun. **25**, 265 (1984)
20. L. Leibler, H. Benoit, Polymer **22**, 195 (1981)
21. D. Cooke, A. Shi, Macromolecules **39**, 6661 (2006)
22. H. Blum, J. Theor. Biol. **38**, 205 (1973)
23. L.R. Nackman, Comp. Graph. Im. Proc. **20**, 43 (1982)
24. N. Amenta, M.W. Bern, *Surface Reconstruction by Voronoi Filtering*, in Symposium on Computational Geometry, (1998), pp. 39–48
25. A. Schoen, Tech. Rep., NASA (1970)
26. E. Sherbrooke, N.M. Patrikalakis, F.E. Wolter, Graph. Mod. Im. Proc. **58**, 574 (1996)
27. S. Hyde, S. Andersson, K. Larsson, Z. Blum, T. Landh, S. Lidin, B. Ninham, *The Language of Shape*, 1st edn. (Elsevier Science B.V., Amsterdam, 1997)
28. H. Schwarz, *Gesammelte Mathematische Abhandlungen. 2 Bände* (Springer, Berlin, 1890)
29. A. Levelut, M. Clerc, Liquid Crystals **24**, 105 (1998)
30. H. Karcher, K. Polthier, Philos. Trans. Roy. Soc. Lond. Ser. A **354**, 2077 (1996)
31. A. Fogden, S. Hyde, Acta Cryst. **A48**, 442 (1992)
32. H. Von Schnering, R. Nesper, Z. Phys. B **83**, 407 (1991)
33. M. Wohlgemuth, N. Yufa, J. Hoffman, E. Thomas, Macromolecules **34**, 6083 (2001)
34. K. Grosse-Braukmann, J. Coll. Interf. Sci. **187**, 418 (1997)
35. S. Lidin, S. Hyde, B. Ninham, J. Phys. France **51**, 801 (1990)
36. W. Gòżdż, R. Holyst, Macromol. Theory Simul. **5**, 321 (1996)
37. B. DiDonna, R. Kamien, Phys. Rev. E **68**, 041703 (2003)
38. B. DiDonna, R. Kamien, Phys. Rev. Lett. **89**, 215504 (2002)
39. T. Ohta, K. Kawasaki, Macromolecules **19**, 2621 (1986)
40. T. Epps, E. Cochran, T. Bailey, R. Waletzko, C. Hardy, F. Bates, Macromolecules **37**, 8325 (2004)
41. C. Hawker, A. Bosman, E. Harth, Chem. Rev. **101**, 3661 (2001), `http://dx.doi.org/10.1021/cr990119u`
42. A. Gray, *Modern Differential Geometry of Curves and Surfaces with Mathematica* (CRC Press, 1998)
43. K. Mecke, *Integralgeometrie in der statistischen Physik* (Harri Deutsch, Frankfurt, 1994)